Pharm Res (2017) 34:654–667
DOI 10.1007/s11095-016-2094-y

RESEARCH PAPER

Preparation and evaluation of biopolymeric nanoparticles as drug delivery system in effective treatment of rheumatoid arthritis

Vijay Kumar[1] • Ankita Leekha[1] • Aakriti Tyagi[1] • Ankur Kaul[2] • Anil Kumar Mishra[2] • Anita Kamra Verma[1]

Received: 26 August 2016 / Accepted: 28 December 2016 / Published online: 17 January 2017

ABSTRACT

Purpose The study purposes to evaluate nanocrystalline biopolymeric nanoparticles encapsulating methotrexate and dexamethasone with high biocompatibility, enhanced therapeutic efficacy and reduced toxicity.

Methods Chitosan nanoparticles were prepared by ionic gelation, and Methotrexate (MTX) and Dexamethasone (DEX) were loaded during the preparation and screened for their *in vitro* efficacy in HEK and RAW264.7 cells, *ex vivo* and *in vivo* efficacy.

Results FTIR confirmed the involvement of phosphoric group of sTPP with amine groups of chitosan and also role of hydrogen bonding involved in the preparation of MTXCHNP and DEXCHNP. Controlled release patterns coupled with diffusion of drug were observed in two different buffers (PBS) at pH 7.4 and pH 5.8. The IC50 for MTXCHNP for HEK was 26.1 μg/ml and 7.7 μg/ml for RAW 264.7 cells. In DEXCHNP, the IC50 was 20.12 μg/ml for HEK and 7.37 μg/ml for RAW264.7 cells. Enhanced uptake of FITC-CHNP by RAW cells indicated internalization of nanoparticles by phagocytosis. The enhanced release of drug at lower pH justified increased cytotoxicity. Negligible *ex-vivo* hemolysis indicated the higher biocompatibility of the nanoparticles. ^{99m}Tc-CHNP exhibited maximum absorption in blood circulation in 3 h, followed by hepatic metabolism and renal clearance. Higher *in-vivo* anti-arthritic activity and antioxidant activity was observed post-intraperitoneal (i.p.) injections by both MTXCHNP and DEXCHNP when compared to MTX (0.75 mg/Kg by i.p. route) and DEX (0.2 mg/Kg/i.p./daily) *per se*.

Conclusion The nanocrystalline biopolymeric nanoparticles were stable, biocompatible and have potential to be administered through i.p. route with minimal toxicity and high efficacy.

KEY WORDS antioxidants · arthritis · biodistribution · chitosan nanoparticles · inflammation

ABBREVIATIONS

DEX	Dexamethasone
DEXCHNP	Dexamethasone loaded chitosan nanoparticles
DLS	Dynamic light scattering
FTIR	Fourier transform infrared spectroscopy
GPx	Glutathione peroxidase
GR	Glutathione reductase
GSH	Reduced glutathione
GST	Glutathione-S-transferase
MTX	Methotrexate
MTXCHNP	Methotrexate loaded chitosan nanoparticles
RA	Rheumatoid arthritis
SEM	Scanning electron microscopy
SOD	Super oxide dismutase
TEM	Transmission electron microscopy
XRD	X-ray diffraction

INTRODUCTION

Biopolymeric nanoparticulate drug delivery systems are fast evolving, as it strategically protects the active molecule from *in vivo* and *in vitro* degradation, reduces the administration rate, enhances circulating levels and therefore, its biological activity may be manipulated for exploiting its therapeutic efficacy. Chitosan, is the only natural polysaccharide that exhibits positive

Electronic supplementary material The online version of this article (doi:10.1007/s11095-016-2094-y) contains supplementary material, which is available to authorized users.

✉ Anita Kamra Verma
akamra23@hotmail.com; akverma@kmc.du.ac.in

[1] Nano Biotech Lab, Department of Zoology, Kirori Mal College, University of Delhi, Delhi 110007, India

[2] Division of Cyclotron and Radiopharmaceutical Sciences, Institute of Nuclear Medicine and Allied Sciences, Delhi 110054, India

charge and, is extensively used for delivery of proteins and nucleic acids. Numerous methodologies of preparation of chitosan nanoparticles using sulfate, citrate and tripolyphospahte have have been published (1). Nanospheres composed of highly concentrated chitosan molecules have also been reported to serve as a "fusogen" (2–4). Small size of chitosan nanoparticles enables it to cross the cell membrane to transport drugs in to the cytosol (5). Owing to their bioadhesive nature, biodegradability and biocompatibility chitosan nanoparticles (CHNP) are accepted as an effective drug delivery system (6–8). CHNP also possess positive charge which enhances its absorption. Also ease of delivery through parentral and non-parentral routes makes it more attractive drug delivery system (9),

Rheumaotoid arthritis (RA), an autoimmune disorder results from interaction between both constitutional and environmental factors (10) causing inflammation of the synovium resulting in joint destruction. RA has also been viewed as a multi-centric tumour-like mass that invades and destroys its micro-environment. Methotrexate (MTX), an antifolate drug, competes with folic acid for binding to dihydrofolatereductase enzyme and blocks the biosynthesis of nucleotides that ultimately result in inhibition of DNA synthesis leading to reduced cell proliferation. MTX is frequently used as a disease modified anti-rheumatic drug (DMARD) for the treatment of RA, alone, or in combination with tumour necrosis factor (TNF) inhibitors (11,12). Clinically, it is also used against human malignancies including acute lymphoblastic leukaemia, breast cancer, malignant lymphoma, osteosarcoma, head and neck cancer. However, being very effective in low doses in RA, MTX is having life threatening complications such as hepatotoxicity, myelosuppression, pulmnory damage (13). Also, Dexamethasone (DEX), a glucocorticoid and first line antirheumatoid arthritic drug is being used in the management of arthritis from a long time. The long term use of DEX results in many complications such as Cushing syndrome, diabetes and bone demineralization, thereby limiting its use (14). Thus, to enhance the efficacy of MTX and DEX with low doses, overcoming their toxicities, we need to deliver MTX and DEX through an efficient biodegradable and biocompatible delivery system.

Since MTX and DEX both are leading drugs used for the management of RA, we have developed CHNP encapsulating MTX and DEX separately. We have further evaluated these nanoparticles in terms of their *in vitro, ex vivo* and *in vivo* efficacy in terms of their cellular studies, biocompatibility, biodistibution studies, antiarthritic and antioxidant potential.

MATERIALS AND METHODS

Materials and Animals

Chitosan (~85% deacetylated, MW ~ 50 kDa), (3-(4,5-dimethyathiazol-2-yl)-2,5-diphenyltetrazolium bromide (MTT), Dimethyl sulphoxide (DMSO), Sodium bicarbonate and HEPES (Hydroxy ethyl piperazine ethane sulphonic acid), 1-Chloro-2,4-dinitrobenzene (DTNB), BSA (Bovine Serum Albumin) were purchased from Sigma-Aldrich (USA). Fetal Calf Serum (FCS), Streptomycin, Penicillin, HPLC water, HPLC methanol were purchased from HiMedia (Mumbai). Methotrexate, Dexamethasone, tripolyphosphate (TPP), β-NADPH, Oxidized glutathione (GSSG) were purchased from MP Bio. The dialysis membrane, Spectra/Por-7; MWCO, (10 kD) was purchased from Spectrum Laboratories Inc (USA). Sodium Dodecyl Sulphate was procured from Bio-Rad laboratories. All the experiments were done using double-distilled and deionized water. Human Embryonic Kidney (HEK) and Mouse macrophage cell line (RAW 264.7) were procured from NCCS, Pune. Wistar rats were procured from AIIMS Delhi.

Synthesis of Chitosan Nanoparticles

Chitosan nanoparticles were synthesized by modifying the earlier protocol of Nogueira *et al.* 2013 (12). Briefly, a premixed solution of sTPP and SDS in a ratio of 2:1 was added dropwise to a 10 ml solution of 0.1% w/v chitosan polymer dissolved in 1% acetic acid solution, under continuous stirring for 30 min at a speed of 500 rpm at pH 5.5. For preparation of MTXCHNP, premixed solution of sTPP, SDS and methotrexate at ratio (2:1:2) was prepared, and was added dropwise to 10 ml of 0.1% w/v chitosan dissolved in 1% acetic acid solution. The experimental conditions were maintained as before and harvested post 30 min. The nanoparticles so obtained were centrifuged and the resulting pellet was washed with acetate buffer and finally resuspended in acetate buffer, lyophilized and further characterized.

For the preparation of Dexamethasone loaded chitosan nanoparticles (DEXCHNP), 1 ml of acetone having 2 mg/ml of Dexamethasone was added to 10 ml solution of 0.1% w/v chitosan polymer dissolved in 1% acetic acid solution and stirred for 30 min. After 30 min, 2 ml of solution having 3 mg of sTPP was added to it dropwise. The solution was stirred at 500 rpm and pH was maintained at 5.5 using 1 N NaOH and harvested post 30 min of agitation. The resulting nanoparticles were centrifuged and the resulting pellet was washed with acetate buffer and finally resuspended in acetate buffer, lyophilized and stored.

For preparation of FITC-CHNP, 5 ml FITC in anhydrous methanol (40%w/v) was further dissolved in 10 ml volume of 0.1% chitosan in 1% acetic acid solution. To this a premixed solution of sTPPand SDS at ratio (2:1) was added, and kept under continuous stirring at 500 rpm at pH 5.5 for 30 min. Further, to remove the free FITC, the solution was centrifuged at 12,500 rpm for 30 min. The pellet was washed by suspending it in distilled water and again centrifuged at

12,500 rpm for another 30 min. Finally, the pellet was dissolved in a known amount of acetate buffer.

Characterization of Nanoparticles

Entrapment Efficiency [%]

Percentage drug entrapment was assessed by calculating the amount of drug trapped in nanoparticles with respect to the total drug that was added during the synthesis of nanoparticles. Briefly, the free drug was quantified by filtering through 0.1 μm syringe filter.

$$\%\ Entrapment\ Efficiency = \left(unfiltered - \frac{filtered}{unfiltered}\right) * 100 \qquad \text{(i)}$$

Drug Content

Drug content of MTX in MTXCHNP was measured by HPLC method with slight modifications (15). Briefly, known amount of perchloric acid was added to MTXCHNP and sonicated. Further this was diluted with the mobile phase, filtered through 0.22 μm capsule filter and run on HPLC having a mobile phase as methanol and PBS (pH6.0) (40:60) using Acclaim 120 (C18, 3 μm, 4.6*150 mm) column with a flow rate 0.75 ml/min. The absorbance was measured at 306 nm for MTX.

The drug content and release kinetics of DEXCHNP were done by in house validated method using Cary 60 UV–vis (Agilent Technologies). 1 ml of prepared nanoparticles were mixed with a known volume of sulphuric acid, the volume was raised upto 3 ml using distilled water. The absorbance was directly observed at 270 nm for DEX and compared with standard.

Size and Zeta Potential

Size and polydispersity index (PDI) of CHNP was determined using Malvern Zetasizer Nano ZS, which works on the principle of Dynamic Light Scattering (DLS). 1 ml of the sample containing nanoparticles was placed in a clear disposable cuvette and the measurement was done using the inbuilt computerized software Zetasizer. PDI gives the narrowness of the particle size distribution (16). Zeta potential was also measured using a zetasizer (Malvern Zetasizer Nano ZS).

Surface Morphology

The morphological assessment in terms of size and shape of CHNP was done by Transmission Electron Microscopy (TEM) and using FEI Tecnai G2 T30 (USA) voltage 300 kV using the preferred magnification. Thin film of nanoparticles was mounted on a carbon-coated copper grid. Grid was then kept in a desiccator to air dry and then loaded on the microscope (17). Scanning Electron Microscopic (SEM) analysis was completed by using EVO LS 10 (Carl Zeiss, Brighton, Germany) scanning electron microscope worked at a working accelerating voltage of 20.0 kV and at high vacuum at amplification of 15000X. The lyophilized samples were dispersed on aluminium stubs using double sided adhesive tape followed by gold bombardment to charge the surface and viewed under the microscope. Smart SEM software program was used to process the image (18).

X-Ray Diffraction Study

Powder X-ray diffraction (XRD) graphs for chitosan, MTX, MTXCHNP, DEX and DEXCHNP were recorded on a Bruker High resolution X-ray diffractometer over the 2θ range of 5–80.

Drug-Excipient Interaction Study

Drug-excipient interaction was investigated using Cary 630 FTIR (Agilent Technologies). The sample was placed on the diamond ATR of the instrument and the peaks were observed using the MicrolabPC software.

In Vitro Release Kinetics

In vitro release pattern of MTXCHNP and DECHNPs was assessed using the dialysis tube method in phosphate buffered saline (pH 7.4 & pH 5.8) (16). Briefly, known amount of nanoparticles were placed separately in dialysis tubes that were immersed in a compartment having 500 ml of media, and stirred at a constant speed of 500 rpm. A sample was taken at regular time points, and the absorbance was recorded at 300 nm (for MTXCHNP) UV–VIS spectrophotometer (Agilent Technologies, USA). The withdrawn sample was further replaced in the beaker so as to maintain the volume. All the experiments were performed in triplicates and the values noted. The analysis of the release kinetics data was done by fitting the data to zero order release, first order release, Higuchi plot and Korsmeyer Peppas models.

Cell Line and Cell Culture

Macrophage cell line RAW264.7 and Human Embryonic Kidney (HEK) cells were maintained in RPMI-1640 supplemented with 10% fetal bovine serum. All the cells were incubated at 37°C in a humidified atmosphere of 5% CO_2 in a CO_2 incubator (Thermo).

Biocompatibility Evaluation

The biocompatibility of MTXCHNP was evaluated by MTT assay (16). Exponentially growing cells were inoculated to 5×10^3 cells/well in a 96 well microplate, cells were supplemented with FCS, 100 IU penicillin and 100 µg streptomycin and incubated with various concentrations of CHNP, MTX, MTXCHNP, DEX and DEXCHNP for 24 h and 48 h. After the requisite time period, 20 µl of MTT solution (5 mg/ml in PBS pH 7.4) was added to each well which result in appearance of Formazan crystals after 4 h of incubation, and were later dissolved in DMSO. The colour was directly proportional to the amount of mitochondrial reduction that indicated the number of viable cells. The optical density for formazan crystals formed was recorded at 540 nm wavelength on an ELISA-reader (SynergyHT, Biotek, USA).

The percent cytotoxicity was determined by

$$\%Cytotoxicity = [A]control - \frac{[A]test}{[A]contol} * 100 \quad \text{(ii)}$$

Where, $[A]_{test}$ is absorbance of the test sample and $[A]_{control}$ is the absorbance of the control sample.

Cellular Uptake

RAW 264.7 cells were seeded in 24 well plates at a density of 10^4 cells/ml and cultured at 37°C in 5% CO_2 for 24 h. Cells were washed with fresh media following incubation of cells with the FITC-CHNP at 37°C in 5% CO_2. After 4 h post-incubation, the cells were again washed with PBS (7.4) and then fixed with 4% paraformaldehyde, further washed thrice with PBS (7.4) and then mounted in Distyrene Plasticizer and Xylene (DPX) and were viewed at a magnification of 20x on a Nikon Eclipse 90i Epi-fluorescence upright microscope equipped with a Nikon DXM 1200 digital camera (19).

Ex-vivo Hemolysis Assay

For hemolytic activity of CHNP, DEX, DEXCHNP, MTX and MTXCHNP, 2 ml of rat blood was collected in EDTA tube. Blood was mixed with equal volume of PBS (7.4), centrifuged at 1500 rpm for 5 min and plasma discarded. The collected blood cells were again washed with PBS (7.4) and supernatant was discarded. The washed red blood cells were diluted with an equal volume of PBS (7.4). 100 µl of these cells was taken in each eppendroff. 100 µl of sample i.e. CHNP, DEX, DEXCHNP, MTX and MTXCHNP were added to each eppendroff. All the eppendroffs were kept at room temperature with continuous stirring on a shaker for 2 h and 4 h respectively. At the end of the 2 h and 4 h of incubation the eppendroffs were centrifuged at 11,000 rpm for 5 min, the supernatant was shifted to a 96well plate and absorbance was measured at 540 nm. The collected data was compared with positive (Triton X) and negative control (PBS 7.4), and percent hemolysis was calculated by formula:

$$\%Haemolysis = \frac{[A]Sample}{[A]\ (+)control} * 100 \quad \text{(iii)}$$

Radiotagging Studies with ^{99m}Tc and Biodistribution Studies

The prepared CHNPs were radiolabeled with technetium-99 m (^{99m}Tc) by direct labelling method as described previously (20). The detailed description of method used is written in supplementary information.

Serum Stability Studies

The *in vitro* serum stability of the ^{99}Tc-CHNP is requisite as serum proteins can cause chelation with the Tc, thereby altering the stability of the nanoparticles. 0.1 ml of the Tc labelled nanoparticles was incubated with the 0.9 ml of serum. The samples were taken at regular intervals and analysed by gamma counter (21).

In Vivo Blood Clearance Studies

Blood clearance study was performed in normal rats ($n = 03$) (20). Briefly, 0.1 ml of radio labelled ^{99m}Tc–CHNP was administered by intraperitoneally (i.p.) to the rats. In pre-weighed tubes, blood sample was collected and counted for radioactivity by gamma counter at different time intervals i.e. 30 min, 1 h, 2 h, 4 h, 21 h and 24 h post i.p. administration. The data was fitted in PK solver to measure the various pharmacokinetic parameters.

In Vivo Biodistribution Studies

Biodistribution studies were performed on adjuvant induced arthritic rats ($n = 03$) post i.p. administration of radiolabeled nanoparticles (^{99m}Tc–CHNP). After i.p. administration ^{99m}Tc–CHNP the animals were sacrificed at different time intervals i.e. 1 h, 2 h, 4 h, and 24 h (20). In pre-weighed tubes, blood samples, and various organs of interest were collected. Radioactivity was counted for each collected organ fraction and expressed as percent administered dose per gram of tissue (% ID per gm) after decay correction.

In Vivo Anti-Arthritic Activity

In vivo anti-arthritic activity of nanoparticles was studied in female wistar rats. The protocol was approved by our

Institutional Animal Ethical Committee (IAEC) having protocol number DU/KR/IAEC/2013/03.

Induction of Arthritis

Adjuvant induced arthritis model was used to develop arthritis in the wistar rats (22). Briefly, 150 µl of Complete Freund's Adjuvant (CFA) was given to right hind paw of rats by intraplantar injection. The control rats were given 150 µl of saline by intraplantar injection. The initial signs of arthritis were visible on the 9th day. From the 10th day, treatment was started and continued up to 30 days.

Treatment Schedule

The rats were weighed and divided in following groups. Group 1, arthritic control was given PBS 7.4 by intraperitoneal route (i.p), Group2 was given MTX *per se* in solution (0.75 mg/Kg by i.p. route), Group 3 was given DEX *per se* in solution (0.2 mg/Kg/i.p./daily), Group 4 was given MTXCHNP in solution having MTX (0.75 mg/Kg/i.p./every third day), Group 5 was given DEXCHNP having DEX (0.2 mg/Kg/i.p./daily), Group 6 was normal control and was given PBS 7.4. For the assessment of arthritis, ankle diameter and paw thickness was measured thrice a week by vernier calliper, and each reading was repeated thrice. The arthritic index of each rat was measured once a week. Both hind paws were carefully given arthritic score on the basis of the onset of inflammation. Arthritis score was given as swelling-1, redness-2, deformity-3 and ankylosis-4.

Antioxidant Activities

Glutathione -S-transferase (GST) Assay

The GST activity was estimated by a slight modification of protocol of Habig *et al.* (23). The detailed method used is given in supplementary material.

Reduced Gluthathione (GSH) Assay

Reduced glutathione estimation was performed by following the protocol of Moron *et al.* (24). The detailed method used is described in supplementary material.

Superoxide Dismutase (SOD) Activity

Superoxide Dismutase assay (SOD) was performed using NWLSS^{TM}Superoxide Dismutase Assay Kit (Northwest Life Science Specialities) as per the manufacturer's instructions.

Glutathione Peroxidase Assay

Glutathione peroxidase assay (GPx) was performed using NWLSS^{TM} Glutathione Peroxidase Assay Kit (Northwest Life Science Specialities) as per the manufacturer's instructions.

Glutathione Reductase Assay

Glutathione reductase (GR), in serum from rats was determined using a modified protocol of Mannervik 2001 (25). The detailed method is described in supplementary material.

Statistical Analysis

All the experiments were performed in triplicates. The graphs and statistical analysis was performed using Graphpad Prism 5 software. Data was compared using One Way ANNOVA and Two Way ANNOVA for Tukey's multiple comparisons test and Bonferroni Posttests respectively.

RESULTS

Preparation and Characterization of Nanoparticles

CHNP, MTXCHNP and DEXCHNP were prepared by ionic gelation method. The EE% of MTXCHNP and DEXCHNP was found to be ~55% and ~10% respectively. Nanoparticles were lyophilized and characterized using DLS. The hydrodynamic size of CHNP, MTXCHNP and DEXCHNP evaluated by DLS was found to be 299.4 nm (PDI 0.437), 217.4 nm (PDI 0.275) and 329.8 nm (PDI 0.286) respectively. Figure 1a represents the DLS study of the prepared nanoparticles.

Further, the surface charge of MTXCHNP (+26.9 mV) and DEXCHNP (+19.5 mV) indicated a decreased zeta potential value as compared to blank CHNP (+35.7 mV) as shown in Fig. 1b. TEM and SEM studies i.e. Figure 1c and d indicated the monodispersity of the nanoparticles having a spherical shape with a diameter around 300 nm.

MTXCHNP and DEXCHNP has found to be crystalline in nature with intense 2Θ values 11.43, 16.95, 19.07, 22.53, 29.74, 33.69, 36.65 and 11.42, 16.94, 19.07, 22.53, 25.07, 29.745, 31.89, 36.84 respectively. MTX and DEX have also crystalline nature with intense 2Θ values as 9.36, 11.55, 12.92, 14.44, 16.06, 17.77, 19.54, 25.52 and 8.66, 11.84, 14.90, 16.14, 17.88, 19.22, 20.33, 22.07, 23.96 respectively. 2Θ value at 20.09 for chitosan governs its partial crystalline nature. Hence, ionic gelation method and coupling of chitosan with MTX and DEX resulted in the formation of a more organised crystal structure in MTXCHNP and DEXCHNP which were also confirmed by TEM diffraction image as shown in Fig. 2.

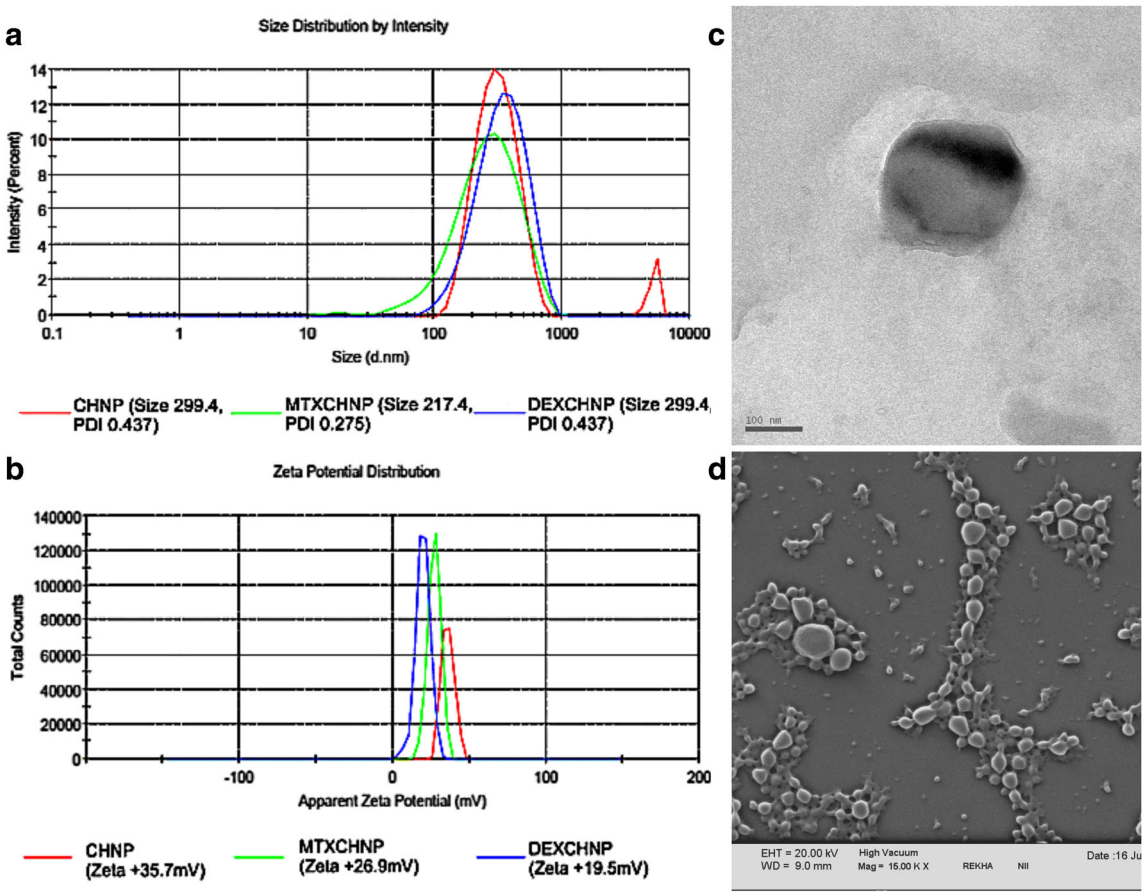

Fig. 1 (**a**) DLS of CHNP, MTXCHNP and DEXCHNP (**b**) Zeta potential of CHNP, MTXCHNP and DEXCHNP (**c**) TEM image of CHNP (**d**) SEM image of CHNP.

FTIR is extensively used to investigate the structure and to analyze the functional groups. The transmission FTIR spectrum of the lyophilized powder of chitosan, MTX, sTPP and MTXCHNP were represented in figure S1 (A). The characteristic peaks for MTX were observed at 3345 c.m^{-1} (−NH stretch), 2928 c.m^{-1} (−CH stretch), 1725 c.m^{-1} (−COOH group), 1648 c.m^{-1} (Amide group), 1603 c.m^{-1} (−NH bending), 1454 and 1543 c.m^{-1} (aromatic ring C=C stretch), confirming the functional groups of MTX. The observed peaks at 3352 c.m^{-1} (−NH stretch), 2876 c.m^{-1} (−CH stretch), 1655 c.m^{-1} (Amide group), 1573 c.m^{-1} (−NH bending), 1067 (−CN stretch), 1030 c.m^{-1} (−C-O stretch), was characteristic to chitosan. The absorption band of –P=O group of sTPP was observed at 1141c.m^{-1}. The characteristic peaks of MTXCHNP were observed at 3410 c.m^{-1} (−NH stretch), 3166 c.m^{-1} (−CH stretch), 1551 c.m^{-1} (−NH bending), 1060 c.m^{-1} (−CN stretch), 1030 c.m^{-1} (−C-O stretch). In MTXCHNP the –NH peak broadens from 3352 c.m^{-1} in chitosan to 3410 c.m^{-1} with increase in intensity, indicating the enhancement of hydrogen bonding. The decrease in –NH bending from 1573 c.m^{-1} to 1551 c.m^{-1} with strong absorption, peak shift of the amide group from 1655 c.m^{-1} to 1648 c.m^{-1} coupled with the absence of -P=O group peak indicated the ionic interaction of chitosan with sTPP and MTX. The interaction between the negative charge of the sTPP and positive charge of the amino group of the chitosan resulted in the formation of nanoparticles. N-H stretching was observed in chitosan that broadens in MTXCHNP. The peak of sTPP reflected that the bond between the chitosan polymer and sTPP were retained in MTXCHNP.

In the spectra of dexamethasone *per se*, the characteristic absorption bands at 3131 and 1260 cm^{-1} were stretching vibration of O-H and C-F bonds respectively as shown in figure S1(B). The stretching vibrations at 1647 and 1593 c.m^{-1} were due to –C=O and double bond framework conjugated to –C=O bonds. Bands at 1450 and 1504 c.m^{-1} (aromatic ring C=C stretch) corresponded to the presence of benzene ring. The observed peaks at 3352 c.m^{-1} (−NH stretch), 2876 c.m^{-1} (−CH stretch), 1655 c.m^{-1} (Amide group), 1573 c.m^{-1} (−NH bending), 1067 (−CN stretch), 1030 c.m^{-1} (−C-O stretch), were characteristic to chitosan. Finally, the overlap of a wide absorption band around 3412 cm^{-1} was due to the stretching vibration of O-H bonded to N-H in DEXCHNP as shown in figure S1(B). The absorption becomes wide with high intensities indicating increased hydrogen bonding in DEXCHNP. Bands at 1552 cm^{-1} and

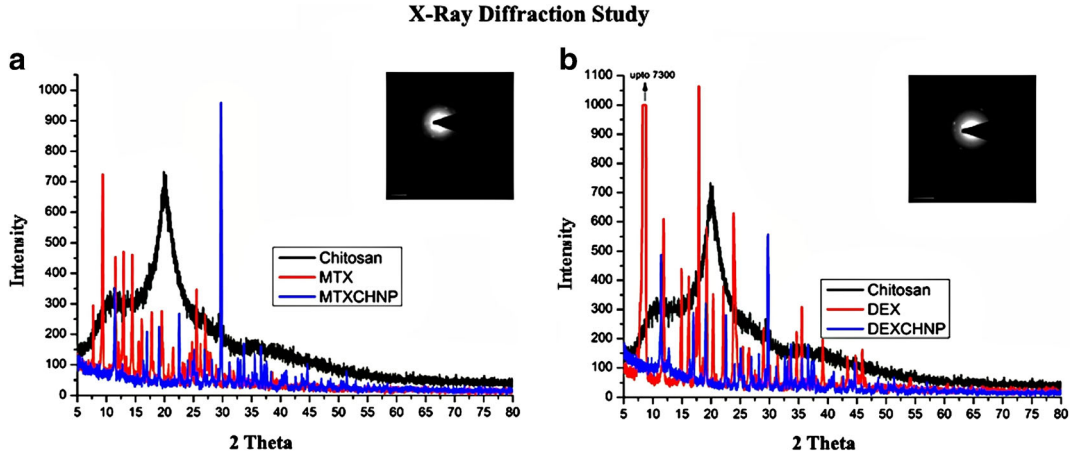

Fig. 2 (**a**) XRD study of chitosan, MTX and MTXCHNP. Inside small image is TEM diffraction image of MTXCHNP (**b**) XRD study of chitosan, DEX and DEXCHNP. Inside small image is TEM diffraction image of DEXCHNP.

1409 cm^{-1} (aromatic ring C=C stretch) corresponded to the benzene ring present. The shifting of peak 3131c.m-1 in DEX to 3412 c.m-1 in DEXCHNP clearly indicating the increased hydrogen bonding involved in the formation of DEXCHNP.

In Vitro Release Kinetics

In vitro release kinetics from MTXCHNP and DEXCHNP at physiological pH 7.4 and arthritic tissue microenvironment i.e. pH 5.8 was studied as shown in figure S2 and S3. MTXCHNP and DEXCHNP both were found to be released with burst effect in first 5 h at both pH conditions. After 5 h high release of drug was observed at pH5.8 than pH7.4. Higher release of drug was observed at pH5.8 than physiological pH7.4 in both the nanoparticles. Data was further fitted in various kinetic models.I It was observed that MTXCHNP followed controlled zero order, Fickian diffusion pattern at physiological pH 7.4 and controlled first order release mechanism at pH 5.8,whereas DEXCHNP followed fast, fickian, first order release at both the pH.

In Vitro Cytotoxicity

The cytotoxic effects of MTX *per se*, void CHNP and MTXCHNP against RAW264.7 and HEK cell line at 24 h and 48 h were verified using the standard MTT assay. It is a non-radioactive assay in which proliferation of cells is assessed by quantifying the amount of MTT reduced, which has direct relationship with the viable cell population. Our results clearly proved time dependent cytotoxicity MTXCHNP against the macrophage cells were greater than the MTX and chitosan *per se*. In normal HEK cell line, we have observed ~18% and ~12% cytotoxicity by MTXCHNP at concentrations of 9.5 μg/ml and 4.75 μg/ml as compared to ~15% and ~11% by free MTX at these concentrations respectively as shown in Fig. 3a. In RAW cell line, higher cytotoxicity was observed at concentrations 9.5 μg/ml and 4.75 μg/ml with MTXCHNP showing ~61% and ~45% cytotoxicity as compared to ~39% and ~49% by free MTX at these concentrations respectively as shown in Fig. 3b. At 48 h more cytotoxicity was observed as compared to 24 h.

The biotoxicity effects of DEX and DEXCHNP on HEK and RAW 264.7 cells at two time points i.e. 24 h and 48 h at two different doses of DEX i.e. 4.75 μg/ml and 9.5 μg/ml, were represented in Fig. 3c and d. DEXCHNP were found to be toxic at both the concentrations on RAW cells while negligible toxicity was observed in HEK cells. Average cellular biotoxicities of DEXCHNP at 24 h were between 3.4 and 17.8% in HEK cells and 41% and 57% in RAW cells evaluated after 24 h, indicating significant uptake of DEXCHNP by the RAW cells. The enhanced sensitivity of DEXCHNP over CHNP and DEX in RAW cells indicated the biotoxicity of the formulation. Also Fig. 3e represents the cellular uptake of FITC labelled CHNP. CHNP were found to be internalized by the RAW 264.7 murine macrophage cells.

Ex-Vivo Hemolytic Activity

Ex vivo hemolytic assay was performed for the determination of biotoxicity and biocompatibility of the prepared nanoparticles with blood. The assay was performed at two different concentrations of CHNP, MTX, MTXCHNP, DEX and DEXCHNP, at two different time intervals i.e. 2 h and 4 h as shown in Fig. 4a. It was observed that CHNP, MTX, DEX, MTXCHNP and DEXCHNP were highly biocompatible ($p < 0.001$) with blood at both the time points i.e. 2 h and 4 h when compared with the positive control at both the time intervals.

Radio Tagging Studies with ^{99m}Tc

The radiolabeling of CHNP with ^{99m}Tc was confirmed by optimizing the labelling parameters such as concentration

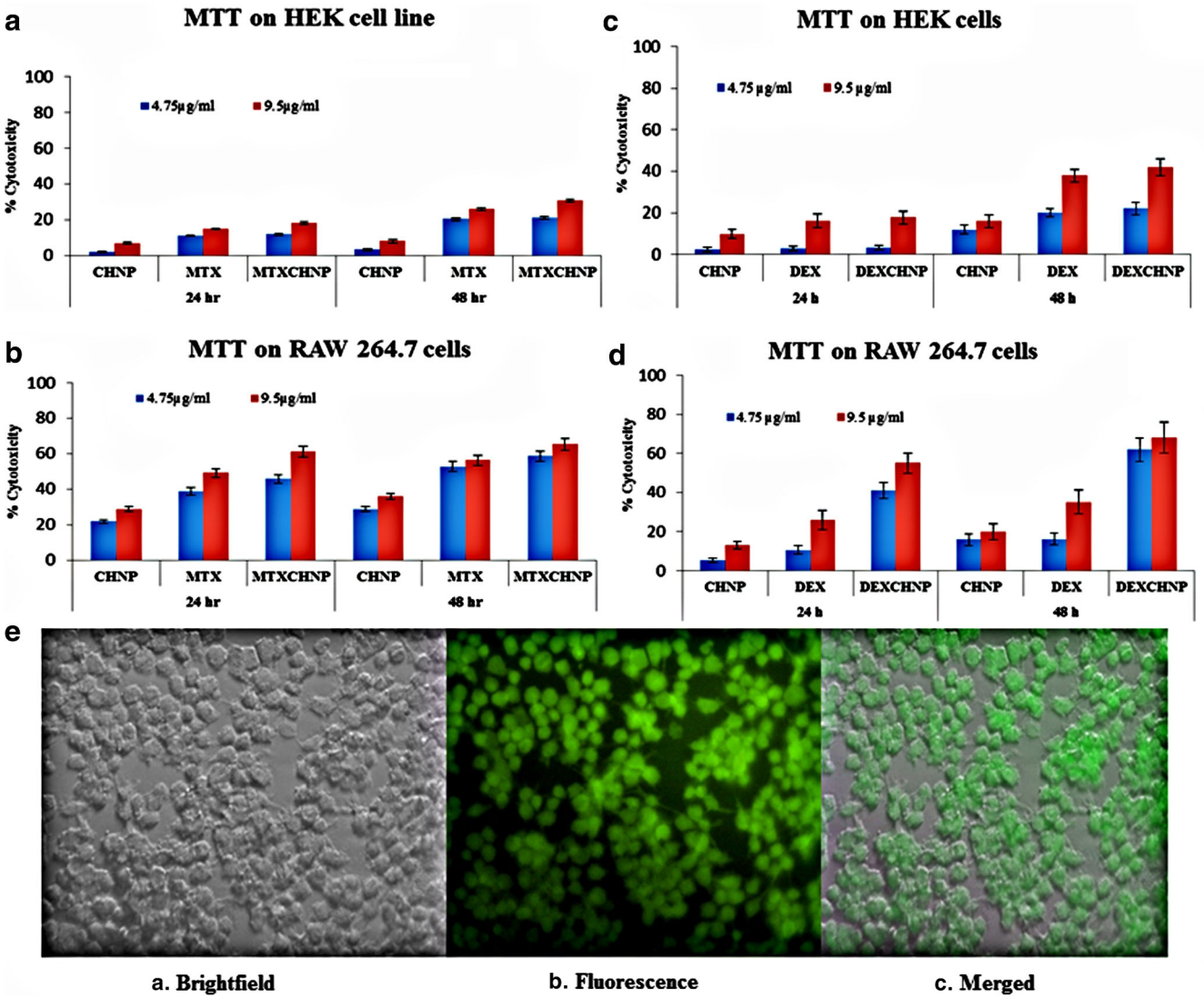

Fig. 3 Cell Cytotoxicity of CHNP, MTX *per se* and MTXCHNP evaluated by MTT assay on (**a**) HEK cell line in 24 and 48 h (**b**) RAW 264.7 cell lines, Cell Cytotoxicity was also evlauted for CHNP, DEX and DEXCHNP using MTT assay in (**c**) HEK cell lines (**d**) RAW 264.7 cells (**e**) *In vitro* uptake of FITC-CHNP by RAW macrophage cells (Mag 40x).

of reducing agent, incubation-time and pH and the radiochemical purity was evaluated chromatographically, which was more than 97%. Even up to 24 h, labelling efficiency was found to be 95.4%, clearly indicating stable radiotagging with CHNP was quite stable and hence could be good candidate for blood kinetics and biodistribution studies.

Serum Stability Study

Mice serum was used to study the *in vitro* proteolytic degradation of the ^{99m}Tc-CHNP. Instant thin layer chromatography of the prepared serum indicated that the nanoparticles remained appropriately stable during incubation at 37°C with the serum. A maximum of 6–7% of radioactivity was found to be degraded after 24 h of incubation (figure S4) advocating a high *in vitro* stability of almost 93% of radiolabelled nanoparticles for up to 24 h.

Blood Kinetics Studies

Blood kinetics parameters were estimated for 24 h and were represented in Fig. 4b. The labelled nanoparticles were found to be absorbed with absorption rate constant (K_a) 2.121. Maximum concentration in blood (C_{max}) was found to be 6.36 at maximum time (t_{max}) 3 h. Post 3 h, the nanoparticles were found to be eliminated with a half-life ($t_{1/2}$) 0.76 h and elimination rate constant (K_{el}) 0.91 h^{-1}. The blood kinetics data of the labelled nanoparticles suggest that the nanoparticles were rapidly eliminated from the circulation. The detailed blood kinetic parameters are depicted in Fig. 4d.

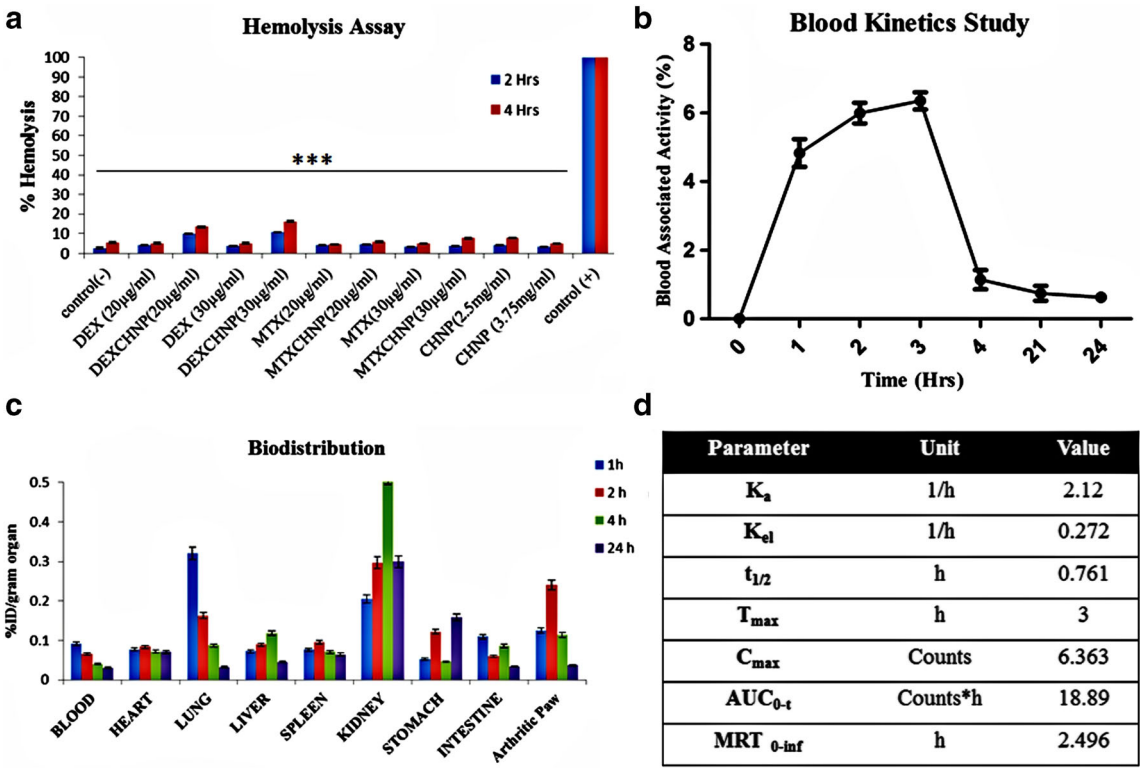

Parameter	Unit	Value
K_a	1/h	2.12
K_{el}	1/h	0.272
$t_{1/2}$	h	0.761
T_{max}	h	3
C_{max}	Counts	6.363
AUC_{0-t}	Counts*h	18.89
MRT $_{0-inf}$	h	2.496

Fig. 4 (**a**) *Ex vivo* hemolysis activity of nanoparticles in 2 h and 4 h. Values are expressed as mean + S.E.M ($n = 3$). *$p < 0.001$, when the treatment groups were compared with the +control. Two way ANOVA Test (Bonferroni Posttests) (**b**) *In vivo* blood kinetics study of ^{99m}Tc-CHNPs ($n = 3$) values are expressed as mean ± S.D. (**c**) Biodistribution studies of ^{99m}Tc-CHNPS at different time intervals i.e. 1 h, 2 h, 4 h and 24 h after interaperitoneal administration (i.p) in adjuvant induced arthritic rat model. (**d**) Blood kinetics parameters calculated using PK Solver DEXCHNP.

Biodistribution Studies

The *in vivo* organ distribution of ^{99m}Tc-CHNPs in adjuvant induced arthritic rats at different time points is represented as a percentage injected dose per gram of tissue (% ID per g) as presented in Fig. 4c.

In Vivo Anti-Arthritic Activity

The swelling in the right paw of the animals induced by CFA injection on the first day increased and sustained till the end of the experiment in the PBS control group. On 10th day rats were divided in to 6 groups and treatment with PBS, MTX, DEX, DEXCHNP and MTXCHNP was started. After 10th days post CFA injection, the first sign of arthritis was observed. Ankle diameter, paw thickness and arthritic score were observed after arthritis was observed on 10th day of CFA injection and measurements were taken every alternate day till the experiment was terminated.

Odema in the right paw was proportional to paw thickness and ankle diameter. It was observed that ankle diameter sharply decreased in MTXCHNP and DEXCHNP treated rats, significantly ($p < 0.01$) when matched with the PBS group on 25th day and 30th day as shown in Fig. 5a. Also, DEXCHNP was found to cure the arthritic rats with a significant difference of ($p < 0.01$) on 30th day. The percentage change in ankle diameter was found to be ~46%, ~47%, 73%, ~65%, ~71% and ~87% for MTXCHNP, DEXCHNP, DEX, MTX, CHNP and PBS group respectively. Positive effect of MTXCHNP and DEXCHNP was observed on paw thickness of diseased rats as both significantly ($p < 0.01$) and ($p < 0.05$) reduced the on 27th and 30th day respectively as shown in Fig. 5b. It was also observed that DEXCHNP reduced the paw thickness of the arthritic rats on 17th and 23rd day significantly ($p < 0.05$) when compared with the control PBS group. The percentage change in paw thickness was ~65%, ~64%, ~76%, ~73%, 87% and ~99% for MTXCHNP, DEXCHNP, DEX, MTX, CHNP and PBS group respectively on 30th day of CFA administration. The relative changes in both paw thickness and ankle diameter clearly indicated the efficacy of MTXCHNP and DEXCHP in recovering the odema of the arthritic rats. Since, arthritis score is the a substantive indicator of the diseased state, the arthritic score of each rat was diligently measured every week post 10th day of the injection till the end of the experiment i.e. 30th day as depicted in Fig. 5c. MTXCHNP group has significantly ($p < 0.05$) decreased the arthritis score on 17th day and ($p < 0.01$) on 30th day of the experiment when compared with the control PBS group. Also, it was further observed that DEX had significantly ($p < 0.01$)

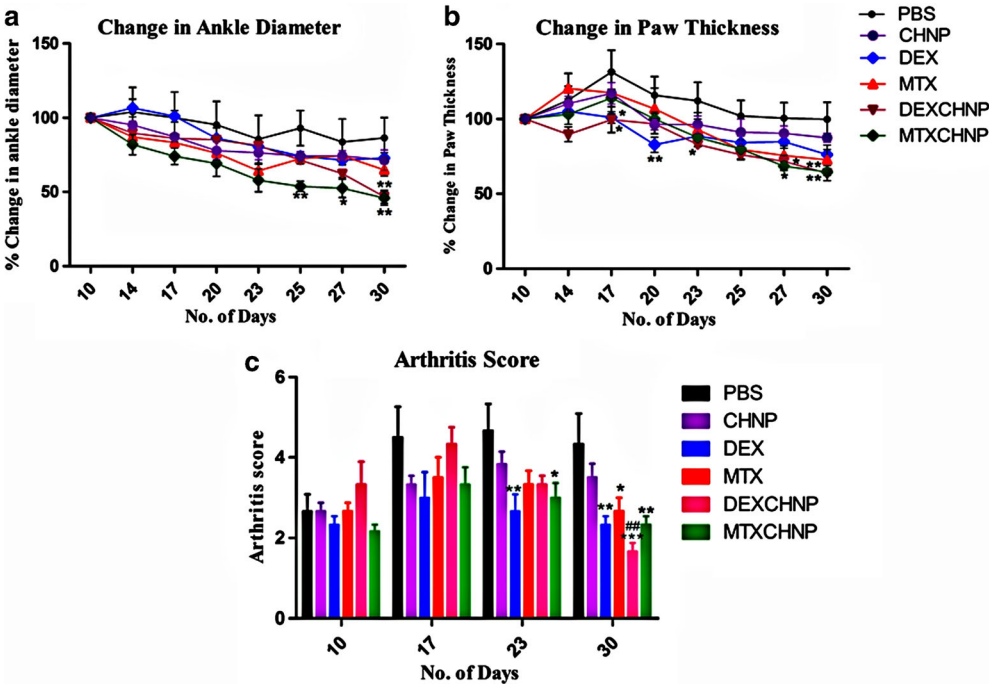

Fig. 5 Effect of CHNP, MTX, DEX, DEXCHNP and MTXCHNP on (**a**) rat ankle diameter (**b**) paw thickness (**c**) Arthritis score on different days after CFA-induced arthritis. **Notes:** Values are expressed as mean ± S.E.M. ($n = 6$ animals/group). *** $p < 0.001$, **$p < 0.01$ and *$p < 0.05$, Two Way ANNOVA (Bonferroni Posttests).

lowered the arthritis score on 23rd day and 30th day of the experiment, whereas, DEXCHNP had lowered the arthritis score very significantly ($p < 0.001$) as compared to the control PBS group. Record of animal images of the different groups were represented in Fig. 6.

In Vivo Antioxidant Assays

Anitoxidant property of a molecule is also a measure of the level of toxicity of the tissues. We have evaluated the effect of Glutathione family enzymes (GST, GSH, GPx and GR) and SOD on 30th day on rat serum. In GST, significant difference ($p < 0.05$) was observed in MTX group (0.73 ± 0.11) when compared with PBS group (1.81 ± 0.57). MTXCHNP lowered the GST values (1.08 ± 0.02) insignificantly from the PBS control group. However, DEXCHNP (3.7 ± 0.11) were found to enhance the GST level significantly ($p < 0.001$) when related with the DEX *per se* (0.91 ± 0.008) and PBS control group as shown in Fig. 7a. The GSH levels of the treated groups i.e. MTX *per se* (20.84 ± 0.43), MTXCHNP (20.06 ± 1.22), DEX *per se* (15.53 ± 2.39), DEXCHNP (25.16 ± 0.84) were similar to arthritic control PBS group (24.16 ± 5.39) as shown in Fig. 7b. However, a significant ($p < 0.001$) variation in arthritic control and treated groups was observed when compared with normal control group (78 ± 2.68). All the treated groups were also found to insignificantly enhance the level of SOD when compared with arthritic control PBS group as shown in Fig. 7c. We have also observed significant ($p < 0.05$) decrease in GR levels in MTX (0.27 ± 0.007) and MTXCHNP group (0.26 ± 0.003) as shown in Fig. 7d. In GPx activity, there was significant variation ($p < 0.001$) observed in DEXCHNP (895.18 ± 95.75) and normal control group (1048.78 ± 20.23) when compared with arthritic control PBS group (299.56 ± 85.28) as shown in Fig. 7e. It was further observed that MTX *per se* (224.23 ± 38.11) and DEX *per se* (192.7 ± 93.67) have GPx levels near to arthritic control PBS group. MTXCHNP enhances ($p < 0.05$) GPx levels when compared with the MTX group. Also, DEXCHNP were found to enhance ($p < 0.001$) GPx levels when compared with the DEX *per se* group.

DISCUSSION

Rheumatoid arthritis (RA), an inflammatory disease that results in debilitating the patient has an extremely challenging treatment regimen.. DMARDs and steroids are the primary choice of medications for RA, but their use is often limited owing to severe toxicity coupled with side effects. To overcome the systemic toxicities, prevention of the degradation of therapeutic agent and to enhance the efficacy of MTX and DEX, we have designed chitosan biopolymeric nanoparticles encapsulating MTX and DEX and evaluated their *in vitro*, *ex vivo* and *in vivo* efficacy.

Chitosan dissolve in acidic pH 5.5, to form a gel to enable preparation of ultrafine nanoparticles in the presence of polyanions such as sTPP exhibiting high zeta potential having an entrapment efficiency for MTXCHNP and DEXCHNP of ~55% and ~10% respectively. The attractive electrostatic interaction between the positively charged chitosan nanoparticles and negatively charged drug molecules at lower pH resulted in increased entrapment of MTX/DEX in the core

Fig. 6 Animal paw images on 30th day of experiment (**a**) MTXCHNP (**b**) MTX (**c**) DEX (**d**) DEXCHNP (**e**) PBS Control.

of chitosan and adsorption on the surface of nanoparticles (12,26). Reduced size of MTXCHNP was observed as compared to CHNP. The decrease in the size of MTXCHNP suggested that, addition of the drug enhanced the degree of nanoparticle compaction (12). The surface charge on MTXCHNP and DEXCHNP decreased, suggesting the saturation of free amino groups of CHNP for the formation of drug loaded nanoparticles. CHNP were found to be spherical in shape as confirmed by TEM and SEM images. FTIR confirmed the reaction of phosphoric group of sTPP with amine

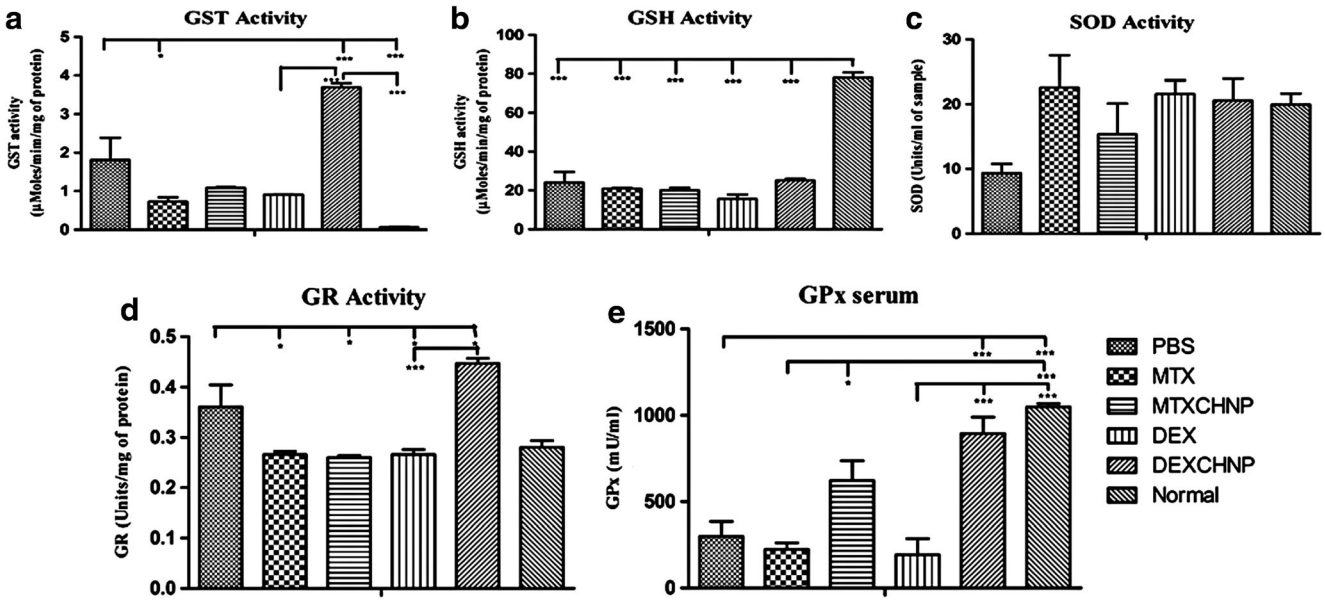

Fig. 7 *In vivo* antioxidant activity of MTX, DEX, MTXCHP and DEXCHNP in serum. (**a**) GST activity (**b**) GSH activity (**c**) SOD activity (**d**) GR activity (**e**)GPx activity. Notes: Data is expressed as mean ± S.E.M. ($n = 6$) ***$p < 0.001$, **$p < 0.01$, *$P < 0.05$ One Way ANOVA using Tukey's Multiple Comparison Test.

groups of chitosan and also involvement of hydrogen bonding involved in the preparation of MTXCHNP and DEXCHNP. X-ray diffraction studies revealed the crystalline nature with sharp peaks in MTXCHNP and DEXCHNP. This crystalline nature of MTXCHNP and DEXCHNP was further confirmed by TEM diffraction studies.

The *in vitro* release behaviour of MTXCHNP and DEXCHNP in PBS pH 7.4 and pH 5.8 was calculated at various time points and was fitted to different release kinetic models (27). MTXCHNP and DEXCHNP both showed fast higher release of drug at pH 5.8. Hence they may have potential to release the drug at inflammatory site with higher rate.

To substantiate whether the nanoparticles were taken up by cells, we studied the uptake of FITC-CHNP in RAW264.7 cell lines. An enhanced cellular uptake was observed in RAW264.7 cell line, as macrophages are phagocytic in nature. Cellular uptake studies (Fig. 3c) indicated that the interaction between charged molecules i.e. negatively charged lipid bilayer of cells and positively charged CHNP may result from various mechanisms like hydrophobic forces, electrostatic forces and in a limited way receptor mediated endocytosis. In contrast to non-phagocytic cells, phagocytic cells preferentially interacted with negatively charged nanoparticles. Simply, counter balancing of the surface charge, cannot be accredited to the entire cytotoxic effects, as both, coating and functionalization distinctly affect the nanoparticle size, that maybe another key constraint for cytotoxicity of nanoparticles. Our results are in unison with the earlier papers, wherein, it is documented that the cells are capable of ingesting positively charged gold and silver particles, lipid particles, chitosan, and polymeric nanoparticles to a higher extent than the respective anionic ones (28). The higher cellular uptake and release of FITC from FITC-CHNP confirmed the fast release behaviour of the CHNP through diffusion mechanism.

Further, we have evaluated *in vitro* cytotoxicity in normal HEK cells and murine macrophage RAW 264.7 cells at 24 h and 48 h. It was observed that MTXCHNP and DEXCHNP showed comparable cytotoxicity for MTX *per se* and DEX *per se* respectively at both time intervals in HEK cells. Hence, a limited uptake of CHNP was observed in HEK cells. The calculated IC50 for MTXCHNP and DEXCHNP for HEK cells was found to be 26.1 μg/ml and 20.12 μg/ml respectively. Furthermore, in RAW264.7 cells, high toxicity was observed by MTXCHNP and DEXCHNP than MTX *per se* and DEX *per se* respectively at both time intervals, which may be directly due to the higher uptake of CHNP by the RAW264.7 cells. The IC50 for MTXCHNP and DEXCHNP in RAW cells was found to be 7.7 μg/ml and 7.37 μg/ml respectively. Our results were unison with the earlier reports, where drug loaded nanoparticles have been reported to be more cytotoxic in RAW cells when compared to MTX (29). The higher uptake of nanoparticles in RAW cells and their higher toxicity at lower doses suggested rapid internalization having potential for RA therapy.

Hemolysis is a standard test to examine the interaction of nanoparticles with the blood components (30). The nanoparticles at the selected doses were biocompatible ($p < 0.001$) with whole blood, as very low hemolysis was observed. With this confidence, we further evaluated the blood kinetics and biodistribution in wistar rats, as *in vivo* model. The radiolabelled ^{99m}Tc-CHNP were found to be quite stable in serum. Blood kinetics showed the absorption of ^{99m}Tc-CHNP in blood circulation. Maximum nanoparticles were in blood circulation post 3 h of injection, which drastically reduced in the 4th h. Maximum accumulation of ^{99m}Tc-CHNP in liver and kidney, was observed in 4 h. Further, the localization of radiolabeled nanoparticles was found to be maximum in kidneys (0.521) at 4 h post injection. Low activity in blood after 3 h reported in blood kinetics study, coupled with higher uptake in kidney and liver confirmed the metabolism of the nanoparticles in the liver followed by renal clearance (21). The enhanced uptake of the nanoparticles at the inflammatory site was observed within 2 h, suggesting accumulation of the nanoparticles at the inflammatory site.

In the *in vivo* adjuvant induced rat arthritis model, MTXCHNP and DEXCHNP significantly reduced the odema and swelling of right foot of the arthritic rats. The higher radioactivity in arthritis paw observed by organ distribution studies further validates the anti-arthritis score findings that the nanoparticles preferentially accumulated in the arthritis paw. During the inflammatory conditions there is continuous production of pro-inflammatory cytokines and reactive oxygen species which further expedite the oxidative stress in arthritic individuals. As a result, there are altered levels of GSH (first line of defence in endogenous oxidant system) and other antioxidant enzymes. We observed reduced GSH, SOD and GPx levels and increased GST and GR levels in PBS control arthritic rats that manifested oxidative damage. Several studies demonstrated altered levels of antioxidant enzyme activities in ROS triggered oxidative stress (31–33). Athough, MTXCHNP and DEXCHNP treatment resulted in negligible change in GSH, the normal levels in serum were observed in SOD and GPx. DEXCHNP resulted in enhanced levels of GST and GR enzymes, hence reduced antioxidant potential. MTXCHNP resulted in decreased GST and GR levels towards normal control, hence, improved antioxidant properties. The enhanced efficacy, biocompatibility and good antioxidant potential made the biopolymeric nanoparticles a suitable system to arrest inflammation and overcome the ailing condition of rheumatoid arthritis.

CONCLUSION

Methotrexate and dexamethasone are widely used antiarthritic drugs that are unable to diminish the arthritic symptoms

completely. Systemic toxicities further limit the aggressive use of these molecules. The encapsulation of these medicines in biopolymeric nanocarriers not only protects them, but also enhances their efficacy by reducing their toxicities. Herein, we have reported the preparation, characterization, release kinetics, *in vitro*, *ex vivo* biocompatibility, blood kinetics, biodistribution, *in vivo* efficacy in adjuvant induced rat arthritic model and antioxidant potential of MTXCHNP and DEXCHNP. Both the nanoparticles were found to be biocompatible with minimal hemolysis, control released, and effective in arresting growth of murine macrophages (RAW264.7), efficient in controlling inflammation in rat arthritic model after intraperitoneal administration by inducing antioxidants. Both the nanoparticles were found to be very effective in RA. Altogether, MTXCHNP and DEXCHNP have anti-arthritic, anti-inflammatory and antioxidant potential that warrant further understanding of the molecular mechanisms involved.

ACKNOWLEDGMENTS AND DISCLOSURES

VK is thankful to Department of Biotechnology, Government of India for JRF, AL and AT received assistance from University Grant Commission. This work was supported by UGC Grant No. F41-35/2012(SR). Authors are thankful to USIC, University of Delhi for providing X-ray Diffraction facility. Authors are also thankful to Mr. Rajeev Kumar for his assistance in animal work.

REFERENCES

1. Jung B, Theato P. Chemical strategies for the synthesis of protein – polymer conjugates. Adv. Polym. Sci. 2012;253:37–70.
2. Fang N, Chan V, Mao HQ, Leong KW. Interactions of phospholipid bilayer with chitosan: effect of molecular weight and pH. Biomacromolecules [Internet]. 2001;2: 1161–8. doi:10.1021/bm015548s.
3. Fang N, Chan V. Chitosan-induced restructuration of a mica-supported phospholipid bilayer: an atomic force microscopy study. Biomacromolecules. 2003;4:1596–604.
4. Huang M, Ma Z, Khor E, Lim LY. Uptake of FITC-chitosan nanoparticles by A549 cells. Pharm Res. 2002;19:1488–94.
5. Van der Lubben IM, Verhoef JC, Borchard G, Junginger HE. Chitosan and its derivatives in mucosal drug and vaccine delivery. Eur J Pharm Sci. 2001;14:201–7.
6. Balkwill F, Mantovani A. Inflammation and cancer: back to Virchow? Lancet. 2001;357:539–45.
7. Illum L, Farraj NF, Davis SS. Chitosan as a novel nasal delivery system for peptide drugs. Pharm Res [Internet]. 1994;11:1186–9. doi:10.1023/A:1018901302450.
8. Zhu BD, Qie YQ, Wang JL, Zhang Y, Wang Q, Zhong, Xu Y, et al. Chitosan microspheres enhance the immunogenicity of an Ag85B-based fusion protein containing multiple T-cell epitopes of Mycobacterium tuberculosis. Eur. J. Pharm. Biopharm. [Internet]. 2007;66:318–26. Available from: http://www.sciencedirect.com/science/article/pii/S0939641106003584.
9. Tiyaboonchai W. Chitosan nanoparticles : a promising system for drug delivery. Naresuan Univ J. 2003;11:51–66.
10. Scholl SM, Pallud C, Beuvon F, Hacene K, Stanley ER, Rohrschneider L, *et al.* Anti-colony-stimulating factor-1 antibody staining in primary breast adenocarcinomas correlates with marked inflammatory cell infiltrates and prognosis. J Natl Cancer Inst. 1994;86:120–6.
11. Thomas TP, Goonewardena SN, Majoros IJ, Kotlyar A, Cao Z, Leroueil PR, *et al.* Folate-targeted nanoparticles show efficacy in the treatment of inflammatory arthritis. Arthritis Rheum. 2011;63: 2671–80.
12. Nogueira DR, Tavano L, Mitjans M, Pérez L, Infante MR, Vinardell MP. In vitro antitumor activity of methotrexate via pH-sensitive chitosan nanoparticles. Biomaterials [Internet]. Elsevier Ltd; 2013;34:2758–72. Available from: http://www.sciencedirect.com/science/article/pii/S0142961213000136.
13. Hoekstra M, Van Ede AE, Haagsma CJ, Van De Laar FJ, Huizinga TWJ, Kruijsen MWM, *et al.* Factors associated with toxicity, final dose, and efficacy of methotrexate in patients with rheumatoid arthritis. Ann Rheum Dis. 2003;62:423–6.
14. Rauchhaus U, Schwaiger FW, Panzner S. Separating therapeutic efficacy from glucocorticoid side-effects in rodent arthritis using novel, liposomal delivery of dexamethasone phosphate: long-term suppression of arthritis facilitates interval treatment. Arthritis Res Ther. 2009;11:R190.
15. Jia M, Li Y, Yang X, Huang Y, Wu H, Hueng Y, *et al.* Development of both methotrexate and mitomycin C loaded PEGylated chitosan nanoparticles for targeted drug codelivery and synergistic anticancer effect. ACS Appl Mater Interfaces. 2014;6:11413–23.
16. Verma AK, Sachin K, Saxena A, Bohidar HB. Release kinetics from bio-polymeric nanoparticles encapsulating protein synthesis inhibitor- cycloheximide, for possible therapeutic applications. Curr Pharm Biotechnol [Internet]. 2005;6:121–30. http://www.ncbi.nlm.nih.gov/pubmed/15853691.
17. Verma AK, Chanchal A, Chutani K. Augmentation of anti–tumour activity of cisplatin by pectin nano–conjugates in B–16 mouse model: pharmacokinetics and in–vivo biodistribution of radio–labelled, hydrophilic nano–conjugates. Int J Nanotechnol. 2012;9: 872–86.
18. Tariq M, Alam MA, Singh AT, Panda AK, Talegaonkar S. Surface decorated nanoparticles as surrogate carriers for improved transport and absorption of epirubicin across the gastrointestinal tract: Pharmacokinetic and pharmacodynamic investigations. Int. J. Pharm. [Internet]. Elsevier B.V.; 2016;501:18–31. Available from: doi:10.1016/j.ijpharm.2016.01.054.
19. Kumar P, Meena R, Paulraj R, Chanchal A, Verma AK, Bohidar HB. Fluorescence behavior of non-functionalized carbon nanoparticles and their in vitro applications in imaging and cytotoxic analysis of cancer cells. Colloids Surf B Biointerfaces [Internet]. 2012;91:34–40. http://www.sciencedirect.com/science/article.
20. Kaul A, Chaturvedi S, Attri A, Kalra M, Mishra AK. RSC advances targeted theranostic liposomes : rifampicin and o fl oxacin loaded pegylated liposomes for theranostic application in mycobacterial. RSC Adv [Internet] R Soc Chem. 2016;6:28919–26. doi:10.1039/C6RA01135G.
21. Mathur R, Bag N, Varshney R, Hussain F, Kaul A, Kumari N, *et al.* Enhanced in vivo tumour imaging by EDTA-bis-GNGR functionalized core shell CdSe:ZnS quantum dot: synergistic effect of active passive targeting. RSC Adv [Internet]. 2016;6:13562–71. http://www.scopus.com/inward/record.url?eid=2-s2.0-84956965700&partnerID=40&md5=4eaaf9107d0a541b3aa46be997496bb3.
22. Shi X-L, Wang L-P, Feng X, Fan D-D, Zang W-J, Wang B, *et al.* Inhibition of adjuvant-induced arthritis by nasal administration of novel synthetic peptides from heat shock protein 65. BMC

Musculoskelet Disord [Internet]. 2014;15:253. https://bmcmusculoskeletdisord.biomedcentral.com/articles/10.1186/1471-2474-15-253.
23. Habig WH, Pabst MJ, Jakoby WB. Glutathione S-transferases. J Biol Chem. 1974;249:7130–9.
24. Moron M, Deoierre J, Mannervik B. Levels of glutathione, glutathione reductase and glutathione S-transferase activities in rat lung and liver. Biochim Biophys Acta - Gen Subj [Internet]. 1979;582:67–78. http://www.sciencedirect.com/science/article.
25. Mannervik B. Measurement of glutathione reductase activity. Curr. Protoc. Toxicol. [Internet]. 2001;Chapter 7:Unit7.2. Available from: http://www.ncbi.nlm.nih.gov/pubmed/23045061.
26. Calvo P, RemunanLopez C, VilaJato JL, Alonso MJ, Remuñan-López C, Vila-Jato JL, et al. Chitosan and chitosan ethylene oxide propylene oxide block copolymer nanoparticles as novel carriers for proteins and vaccines [Internet]. Pharm. Res. 1997;1431–6. doi:10.1023/A:1012128907225.
27. Ti li Aydin RS, Pulat M. 5-fluorouracil encapsulated chitosan nanoparticles for pH-stimulated drug delivery: evaluation of controlled release kinetics. J. Nanomater. 2012;2012.
28. Fröhlich E. The role of surface charge in cellular uptake and cytotoxicity of medical nanoparticles. Int J Nanomedicine [Internet]. 2012;7:5577–91. Available from: http://www.pubmedcentral.nih.gov/articlerender.fcgi?artid=3493258&tool=pmcentrez&rendertype=abstract.
29. Moura CC, Segundo MA, DasNeves J, Reis S, Sarmento B. Co-association of methotrexate and SPIONs into anti-CD64 antibody-conjugated PLGA nanoparticles for theranostic application. Int J Nanomedicine. 2014;9:4911–22.
30. Dobrovolskaia MA, Clogston JD, Neun BW, Hall JB, Patri AK, Mcneil SE. Method for analysis of nanoparticle hemolytic properties in vitro 2008. 2008
31. Gelderman KA, Hultqvist M, Olsson LM, Bauer K, Pizzolla A, Olofsson P, et al. in Disease development and therapeutic strategies. 2007;9.
32. Sharma S, Sahu D, Rani H, Sharma D. Amelioration of collagen-induced arthritis by Salix nigra bark extract via suppression of pro-inflammatory cytokines and oxidative stress. Food Chem. Toxicol. [Internet]. Elsevier Ltd; 2011;49:3395–406. doi:10.1016/j.fct.2011.08.013.
33. Sundaram MS, Hemshekhar M, Santhosh MS, Naveen S, Devaraja S, Rangappa KS. Tamarind Seed (Tamarindus indica) Extract Ameliorates Adjuvant- Induced Arthritis via Regulating the Mediators of Cartilage/Bone Degeneration, Inflammation and Oxidative Stress. Nat. Publ. Gr. [Internet]. Nature Publishing Group; 2015;1–13. doi:10.1038/srep11117.